Electrospinning of ultrafine non-hydrolyzed silk sericin/PEO fibers on PLA : a bilayer scaffold fabrication

Paul Mathieu, Rémi Bascou, Francisco Sebastian Navarro Oliva, Alla Nesterenko, Anh-Tu Ngo, Isabelle Lisiecki, Erwann Guénin, Fahmi Bedoui

Electrospinning of ultrafine non-hydrolyzed silk sericin/PEO fibers on PLA : a bilayer scaffold fabrication

Paul Mathieu[1,2], Rémi Bascou[2], Sebastian Navarro Oliva [1], Alla Nesterenko[2], Anh-Tu Ngo[3], Isabelle Lisiecki[3], Erwann Guénin[1,2], Fahmi Bedoui[1]*

[1] *Centre de Recherche de Royallieu, Roberval Laboratory for Mechanics, CNRS, Université de Technologie de Compiègne, 60203 Compiegne, France.*

[2]*Université de Technologie de Compiègne, ESCOM, TIMR (Integrated Transformations of Renewable Matter), Centre de Recherche Royallieu-CS 60 319-60 203 Compiègne Cedex, France*

[3]*Sorbonne Université, CNRS, De la Molécule Aux Nano-Objets: Réactivité, Interactions Spectroscopies, MONARIS, Paris, 75005, France*

**Corresponding author.*

E-mail address : fahmi.bedoui@utc.fr

Keywords : Electrospinning, Bilayer scaffolds, Silk Sericin, Polylactic Acid, Nano-fibers.

Abstract

Here we report the feasibility of electrospinning of protein-polymer multilayered scaffolds with selected materials such as non-hydrolyzed silk sericin (SS), polyethylene oxide (PEO) and polylactic acid (PLA), with tuned fiber size and properties for each layer. We present a new innovative way for the electrospinning (ES) of non-hydrolyzed SS mixed with PEO yielding fibers with an average diameter ranging between 120 nm and 150 nm. Different SS:PEO ratios have been electrospun to study the effect of the concentration of silk sericin protein on the fibers size and shape, as well and their electrospinnability. Electrospun SS:PEO fibers display weak to no mechanical resistance (non-measurable) their deposition onto a sturdier scaffold is necessary to allow their use in biomedical and/or pharmaceutical fields. Therefore, bilayer scaffolds have been fabricated consisting of a PLA support and SS:PEO fibers obtained from the optimized SS:PEO ratio (1.2:4). They are composed

of a sturdy hydrophobic layer of PLA fibers and a layer of sticky hydrophilic SS:PEO fibers. The scaffolds have been characterized extensively by Fourier Transforms Infra-Red (FTIR) spectroscopy, X-Ray diffraction (XRD), Scanning Electron Microscopy (SEM) and their resistance to mechanical stress. Finally, hydrophobicity of both layers has been determined by measuring the contact angle of water droplets on the scaffolds, further proving the bilayer nature of the scaffolds.

1. Introduction

Electrospinning is a versatile technique able to produce films made of entangled fibers with wide range of diameters from micro to nanometer scale [1]. This nanometric fiber size presents many interests for different fields of applications such as tissue engineering [2–5], energy [6,7], healthcare [8,9], protective clothing [10,11], filtration [12] and so on. This versatility comes from the wide range of different polymers that can be electrospun, with controlled size and shape which are tunable for the desired applications [13–16]. For biomedical applications and tissue engineering, the electrospun non-woven nanofibrous mimics the extracellular matrix much more efficiently compared to conventional techniques [2–5]. Nanoscale fiber can also be used as a drug delivery system. Dissolving the drug of interest in a polymer solution followed by the electrospinning of the mixture leads to drug loaded fibers [8]. In the field of energy, the high surface to volume ratio, low density and high porosity of electrospun fibers make them a good candidate in energy devices [6]. In addition to versatility, ES presents another advantage which is flexibility and simple experimental setup requiring only a high voltage generator, a syringe pump and a collector.

Silk Sericin (SS), is a biomass derived protein mainly composed of serine, aspartic acid and glycine amino acids [17], it also constitutes up to 30% of the silk cocoons (from *Bombyx Mori*). Silk cocoons contains mainly fibroin, widely used in the textile industry, but the extracted SS during the fabrication of silk fibroin is usually considered as a waste [17,18]. Properties of SS such as antimicrobial effect, resistance to UV, moisture absorption as well as their ability to polymerize and copolymerize to form various types of composites, makes it a very promising product for different types of application in biomedical and pharmaceutical fields [19–23]. Electrospinned SS has a

particular interest in biomedical application for tissue engineering and particularly wound dressing and the reparation of epithelial tissues [17,24]. In addition, the presence of fibers and thus porosity is particularly important in the wound dressing application as reported by Bakhsheshi *et al.* [25].

The primary way to electrospin SS was to use preparation of sericin peptides obtained from hydrolysis of the whole sericin protein [26] but these techniques may lead to a loss of the intrinsic properties of the entire protein (structuration, molecular weight, glue properties). The second way is to exploit the whole SS protein and to mix it with another polymer. Such a strategy is widely used for the electrospinning of the other major silk protein: fibroin [27]. PEO is often utilized as a copolymer as it is non-toxic, soluble in water and partially prevents spontaneous gelation of such proteins in concentrated solution. To electrospin SS in water, the only polymer that have been used so far is polyvinyl alcohol (PVA). Eslah *et al.* [28] reported the elecrospinning of PVA/SS fibers with different ratios (90:10, 85:15, 80:20 and 75:25). The fibers obtained had a size ranging from 365 nm to 426 nm. In this work the authors reported the difficulty to electrospin solutions for ratios of SS above 20 % because of the gelation of the polymer blend. Other electrospinning of a mixture of PVA/SS/Clay have been reported by Purwar *et al.* [20,21], where they describe fiber diameter sizes reaching down to 150 nm.

We decided to undertake the electrospinning of pure non-hydrolyzed SS in order to estimate the feasibility of making pure SS fibers of controlled diameter. But, extraction and electrospinning of non-hydrolyzed SS protein still presents a challenge, as the SS macroscopic and microscopic properties differs with the techniques of extraction which are numerous [17,29–33]. Therefore, in this work we undertake the electrospinning of mixed non-denaturized silk sericin (SS) with polyethylene oxide (PEO) fibers. Effect of non-denaturized SS concentration on the fibers size and shape is evaluated and bilayer scaffolds on a polylactic acid (PLA) electrospun mats are produced. At the best of our knowledge, there are no current published work on the electrospinning of non-hydrolyzed SS:PEO fibers, or even using the whole SS protein in the literature.

2. Materials and method

2.1 Materials

PLA was purchased from Natureplast (Pli 003), 2,2,2-Trifluoroethanol (TFE, > 99%) and Polyehtylene oxide (PEO MM=900 kDa, Mv ≈ 900.000) were purchased from Sigma Aldrich. Bombyx mori silk cocoons were obtained from "Au fil d'Emma" (SC0050), France.

2.2 Syntheses

2.2.1 Extraction of SS

The methodology of non-hydrolyzed SS extraction was optimized in our laboratory recently, and details are published elsewhere [34]. Briefly, 12.2 grams of silk cocoons are cut to around 5mm pieces and put in 305 mL of deionized water in an autoclave bottle. A cycle of sterilization is then set for 120 °C for at least 40 minutes in an autoclave. After the extraction the mixture is then sonicated for 5 minutes and followed by a filtration with a Büchner. At this stage, 270 mL of solution is obtained with approximatively 1% w/v of SS. Addition of 12 mL of LiBr at 9.3 M is followed by the evaporation of the solution to concentrate the SS. Diminution from 270 to 80 mL yielded a solution of 3 % SS. The obtained jelly/liquid solution is then dialyzed (membrane 3500 MWCO) in milliQ water (18.2 MΩ) for 48 hours with water change every 12 hours for salt elimination.

2.2.2 Preparation of the SS:PEO solutions

The SS and PEO solutions were prepared by using the 3% (w/v) SS solution previously prepared. The 3% SS solution was diluted by adding a 6% w/v PEO solution and milliQ water (18.2 MΩ) until the wanted ratios of 1:10, 1:5, 1.2:4 and 1:2 between SS and PEO were obtained. Final w/v% of PEO is kept at 4%, while the amount of sericin changes from 0.4% to 2%. The solutions were then stirred at 70°C in closed vials until homogenous, for roughly 2-4 hours.

2.3 Electrospinning

2.3.1 PLA scaffolds

A 25% (w/v) polylactic acid (PLA) solution was prepared by dissolving PLA pellets in 2,2,2-trifluoroethanol by heating at 60 °C and magnetically stirring overnight in a closed vial. The PLA

solution was then transferred in a 10 mL plastic syringe (BD Plastipak, in polypropylene) attached to a 18G blunt tip needle. The collector was covered by a piece of aluminum foil from Fischer brand (thickness of 0.024 mm). The syringe was then loaded onto an automatic syringe pump and a flow rate of 16 µl/min was set. The distance between the tip and the collector was set at 18 cm while a constant potential of 18kV was applied throughout the collection of the scaffold with a custom-built high voltage generator. The volume of injection was set a 0.32 mL for a total collection time of 20 minutes per scaffold. The obtained scaffold was then removed from the aluminum foil and analyzed by IR, SEM, XRD and water contact angle.

2.3.2 Electrospinning of SS:PEO fibers

The SS:PEO solution was then transferred in a 10 mL syringe (BD Plastipak, lure lock) attached to a 18G blunt tip needle. The collector was then covered with aluminum foil (Fischer Brand, 0.024 mm thickness) to allow analysis of the obtained fibers. The syringe was then loaded onto a syringe pump and the flow rate was set to 10 µl/min depending on the SS:PEO ratio electrospinned. The distance between the tip of the needle and the collector was set at 14 cm, while a 10 kV to 21 kV current was applied throughout the whole process with a custom-built electrical generator. Electrospinning of 0.6 mL during one hour allowed the collection of SS:PEO fibers on the aluminum foil.

2.3.3 Electrospinning of PEO fibers

A 5% w/v solution of PEO in water was prepared by dissolving 500 mg of PEO in 10 mL of water by heating and magnetically stirring the solution for 48h at 70°C in a closed vial. The 5% PEO solution was then transferred in a 10 mL syringe attached to a blunt tip needle. The collector was then covered with aluminum foil (Fischer Brand, 0.024 mm thickness). The syringe was then loaded onto a syringe pump and the flow rate was set between 16.6 µl/min (1mL/h). The distance between the tip of the needle and the collector was set at 18 cm, while a 12.5 kV current was applied throughout the

whole process with a custom-built electrical generator. Electrospinning of 0.6 mL during 30 minutes allowed the collection of a PEO scaffold on the aluminum foil.

2.3.4 Electrospinning of bilayer scaffolds PLA/SS:PEO

After the PLA electrospinning, the aluminum foil bearing the scaffold was taped of the collector prior to the electrospinning of the SS:PEO fibers. The wanted SS:PEO solution was then loaded in a 10mL syringe attached to a blunt tip needle. The syringe was then loaded onto a syringe pump and the flow rate was set to 10 µl/min. The distance between the tip of the needle and the collector was set between 10 cm and 14 cm, while a 10 kV to 21 kV current was applied throughout the whole process with a custom-built electrical generator. Electrospinning of 0.6 mL during one to five hours allowed the collection of SS:PEO fibers on the aluminum foil.

2.4 Measurements

For SEM analysis, samples were cut in squares (approximately 5 × 5 mm) out of the electrospun film, mounted on carbon discs, and observed using a Quanta FEG 250 from FEI Environmental Scanning Electron Microscope (SEM). The size distributions were acquired by measuring a minimum of 250 objects using the open source ImageJ software. Sizes are given as mean ± standard deviation according to a Gaussian fit of the corresponding size distribution.

IR spectra were recorded in ATR (attenuated total reflection) mode on a Thermo scientific Nicolet iS5 Infrared Spectrophotometer. All spectra were recorded in solid state in a range of 400 cm^{-1} to 4000 cm^{-1}.

XRD analysis were performed using a Bruker D8 Advance diffractometer with X-ray wavelength of 0.1542 nm, operated at 30 kV and 40 mA. The scanning covered the 2Θ range of 5° to 70 ° with steps of 0.02°.

The contact angles of water on the electrospun samples were measured by using a Drop Shape Analysis system Krüss DSA10 (Hamburg, Germany) at room temperature (20 ± 3 °C). A drop of deionized water was placed perpendicularly onto sample surface. Then, the images of drops were

recorded and analyzed using the tangent method. The final result for each sample was obtained by averaging the values of at least three measurements.

Mechanical tests were run on a tensile micromachine (DEBEN microtest system) using 2 cm x 0.5 cm stripes of each scaffold. The testing was operated at a permanent elongation speed of 1 mm/min.

3. Results and discussion

Electrospinning of a bilayer scaffold have been undertaken. The main purpose of a bilayer is to obtain different properties for each side of the scaffold. Electrospinning of PLA allows the synthesis of hydrophobic fibers, while electrospinning of sericin yields hydrophilic fibers. Combination of both scaffolds into a unique bilayer would be most interesting in the field of wound dressing, or to create patches.

3.1 Electrospinning of SS:PEO fibers

The electrospinning of pure PEO (5% w/v) as inspired by the work of Belda Martin *et al.* [27] was undertaken to analyze the fabrication of the fibers and film without the effect of the SS. Electrospinning of the PEO for two hours yielded a fragile scaffold of PEO. The SEM analysis displays the presence of fibers of around 200 nm of diameter (**Fig 1.a**). Compared to the reported fibers of Jacobs *et al.*, our pure PEO electrospun fibers displays much less defaults, but with an increased fiber diameter [35]. Then, electrospinning of pure non-denaturized SS have been undertaken. Unfortunately, from a concentration from 0.5 % to 3 % w/v of SS in water, no electrospinning is possible, which can be the consequence of highly gelatinous aspect of the solution. Then, evaluation of electrospinnability of SS:PEO mixture were conducted at low concentration of SS *v.s.* PEO in the solution by keeping the w/v percentage of the PEO in the final solution at 4 % as inspired by Belda Martin work [27]. Different ratios of SS:PEO have been attempted to be electrospinned: 1:10, 1:5, 1.2:4 and 1:2 ratios and all electrospinning conditions have been reported in **Table 1.**

Table 1

Electrospinning conditions of SS:PEO solution of different ratios

SS:PEO ratio (Total w/v % of SS+PEO in solution)	*Voltage*	*Tip to collector distance*	*Flow rate (mL/h)*	*Average fiber diameter (nm)*	*Defects*
1:0 (3%)	*Not possible to electrospin (from 0.5% to 3% w/v)*				
1:10 (4.4% w/v)	*10 kV*	*14 cm*	*0.6 mL/h*	-	*Beads and droplets*
1:5 (4.8 % w/v)	*12.5 kV*	*14 cm*	*0.6 mL/h*	-	*Beads and droplets*
1.2:4 (5.2 w/v)	*17 kV*	*14 cm*	*0.6 mL/h*	*121.4 ± 44.9 nm*	*Few to none*
1:2 (6% w/v)	*21 kV*	*14 cm*	*0.6 mL/h*	*139.2 ± 59 nm*	*Few to none*
0:1 (5% w/v)	*12.5 kV*	*18 cm*	*1mL/h*	*272 ± 123.9 nm*	*Beads*

After one hour of fabrication a thin layer of product or fibers have been collected on the taped aluminum foil. SEM micrographs for the depot obtained from the 1:10 ratio of SS:PEO show very thin fibers (around 80 nm) with a majority of defaults (beads and droplets) as shown in **Fig. SI.1**. Similarly, SEM micrographs of the deposition obtained from the 1:5 ratio shows almost no fibers at all with a majority of beads and droplets (**Fig. SI. 1**). The obtained depot is more comparable to electrospraying than electrospinning with almost no fibers observable.

Electrospinning of SS:PEO with higher ratio of SS were then undertaken to study the effect of higher SS concentrations. Electrospinning of the SS:PEO solution (ratio 1.2:4) was performed with a needle an optimized tip to collector distance of 14 cm and 17 kV voltage applied and electrospinning of a solution of SS:PEO (ratio 1:2) with a needle tip to collector distance of 14 cm and 21 kV voltage

applied. After one hour of fabrication at a rate of 0.6 mL/h, a thin layer of fibers is obtained on the aluminum for each solution.

For the 1.2:4 SS:PEO ratio, SEM micrographs (**Fig. 1.b**) display fibers with an average diameter of 121.4 ± 44.9 nm with very few defaults to note (beads). For the higher ratio 1:2 SS:PEO fibers the size remains similar with a mean diameter of 139.2 ± 59.0 nm (**Fig. 1.c**). These results show that SS:PEO fibers of different sericin content can be obtained by electrospinning. Moreover, fibers of different diameter can be obtained while changing the concentration of non-denaturized SS content from 23 % to 33 % in the final product (size increasing from 121 nm to 139 nm). Average size of the fibers in both scaffolds are thinner than those reported by Bakhsheshi *et al.* [25] with an average size reaching 300 nm and comparable in size to the fibers reported by Purwar *et al.* [20]. In both cases the electrospun scaffolds were too fragile and too sticky to be removed for the aluminum foil support and thus could not be analyzed in XRD. Finally, compared to the pure PEO fibers, the SS:PEO fibers show less defaults and have a narrower size and dispersity (**Fig. 1.a**).

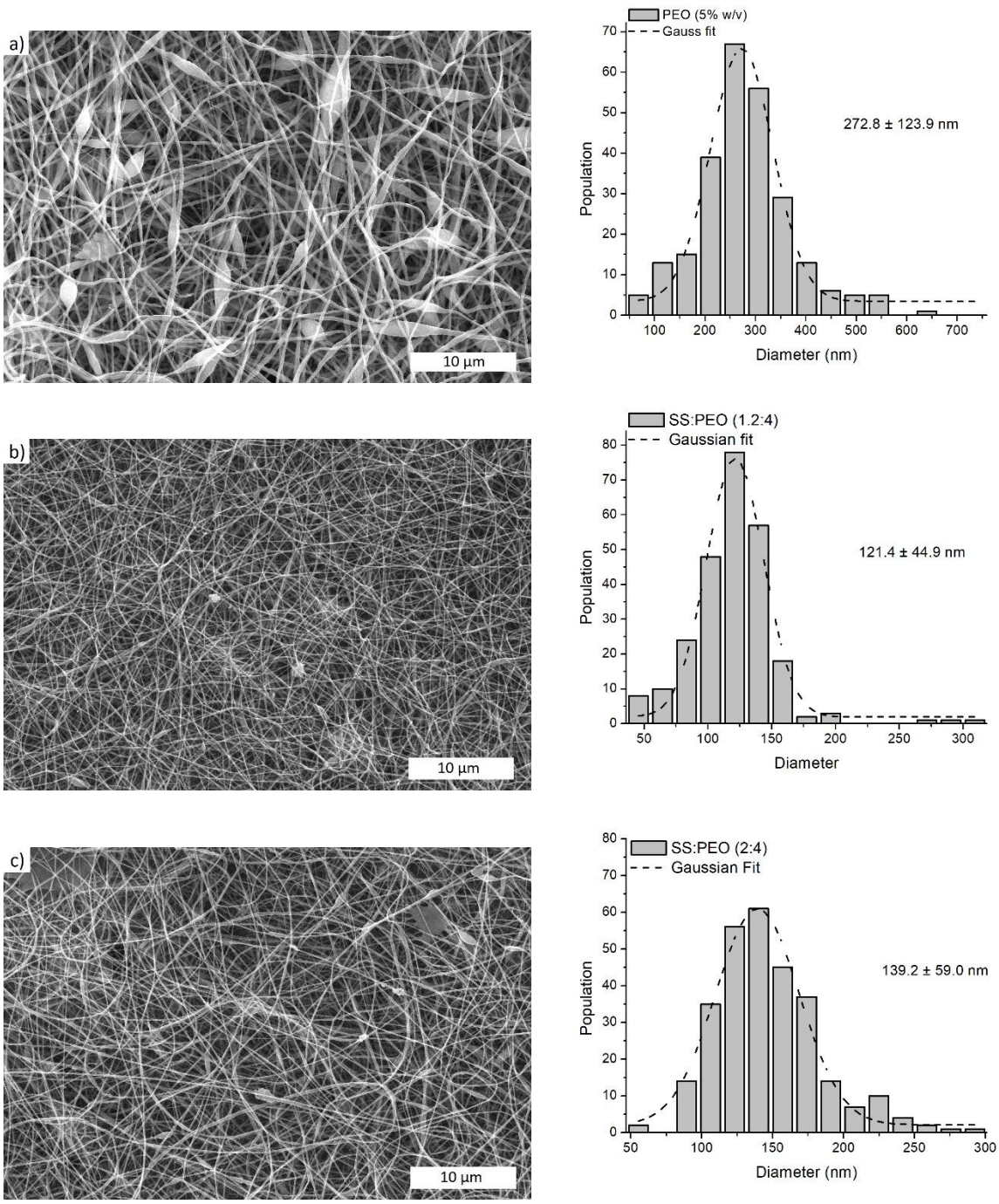

Fig. 1. SEM micrographs of and their according size distribution of a) PEO (5% w/v) electrospinned fibers b) SS:PEO (1.2:4) fibers and c) SS:PEO (1:2) fibers.

3.2 Electrospinning of bilayer scaffolds

3.2.1 Electrospinning of PLA scaffolds

PLA is a low-toxic and fast biodegradable polymer that have shown great potential especially in the biomedical field [36,37]. We chose to use this polymer to constitute the support film for the SS:PEO fibers, because of the difference of behavior towards water (SS:PEO is hydrophilic). Most of the recent work for PLA used DMF mixed with another solvent (usually acetone, chloroform, dichloromethane) [38]. Here, we report the electrospinning of PLA in 2,2,2–trifluoroethanol (TFE) as inspired by Gomez-Pachon *et al.* [39]. Although this solvent is toxic, unlike DMF it is easier to dry and thus to remove the remaining traces of solvent in the fibers without heating the scaffolds. Electrospinning of a 25% w/v solution of PLA in TFE was undertaken at a flow rate of 1mL/h with a needle tip to collector distance of 18 cm and a voltage of 11 kV. After 20 minutes of ES, the obtained fibers displays a mean size around 1000 nm with few defaults to note (some beads and pearls) as shown on the SEM micrographs (**Fig. 4.a**).

3.2.2 Bilayer scaffolds of PLA and SS:PEO

To overcome the fragility of the SS:PEO scaffolds, the deposition of these fibers on the sturdier previously electrospun PLA base have been studied. To obtain the bilayer scaffold, ES of SS:PEO (1:2) has been selected because of the reproducibility of the ES process and the high percentage of sericin in the fibers (33%).The alumium foil supported PLA scaffold is then taped again on the collector and collection of the SS:PEO (1:2) fibers is undertaken at a distance of 14 cm between the tip of the needle and at a voltage of 21 kV. After two hours of electrospinning, the scaffold is then detached from he aluminum foil and analyzed in SEM, XRD, IR analisys of the SS:PEO side and PLA side of the scaffolds. This revealed that two different type of fibers are present. On the the PLA side the size of the fibers ranges from 300 nm to 700 nm (**Fig 4.b**). And on recto side (with SS:PEO) the fibers have a diameter of 182 ± 246 nm (**Fig 4.c**). The difference between the SEM micrographs on both sides is the first proof of the bilayer nature of the scaffolds fabricated with the presence of SS containing fibers

However the creation of the bilayer has proven to be non reproducible especially for the 1:2 SS:PEO electrospinning process with poor microstructure and almost no SS:PEO fibers observable. The gelatinous texture of the 1:2 SS:PEO solution might be the origin of the bad reproducibility of the bilayer electrospinning process since the ES is sensitive to ambient humidity and temperature. To try to overcome this problem, electrospinning of the 1.2:4 ratio of SS:PEO fibers was also undertaken on a PLA film previously electrospun. After one hour of electrospinning at a rate of 0.6 mL/h with a needle tip to collector distance of 10 cm and 15 kV voltage applied, the bilayer scaffold is analyzed by SEM, IR and XRD. SEM analysis shows a uniform repartition of the SS:PEO fibers on top of the PLA fibers, with an average diameter ranging from 100 nm to 300 nm on the SS side (**Fig. 4.d**). Similar bilayer scaffolds are reported by Zhao *et al.* [40] by electrospining PLLA/SS for wound dressing. However, in their work, the electrospinning process consisted in the use of trifluoroacetic acid for the elctrospinning of the sericin, and peptides of SS instead of the whole SS protein. Then, study of the hydrophobic/hydrophilic properties of the two different layers have been then undertaken and are reported in the **Table SI. 1**. The hydrophilic-hydrophobic character of electrospun samples was evaluated by contact angle measurements. As expected, the SS containing sample diplays the most hydrophilic properties mainly because of the presence of serine hydroxyl groups and aspartic acid carboxyl groups allowing an increased affinity with water via hydrogen bonds formation. On the other hand, PLA sample posseses hydrophobic properties with a contact angle of 121.6 ± 0.18 ° due to the presence of methyl group (**Fig. 2**). The results show that samples PLA/SS:PEO present intermediate value of contact angle 70.4 ± 0.4 ° for PLA/SS:PEO (1.2:4) and 110.16 ± 0.51 ° for PLA/SS:PEO (1:2) which confirms the bilayer nature of the scaffolds (**Fig. 3**). The results indicate that obtained bilayer scaffolds have adjustable wettability. This can be particularly useful for biomedical applications such as bio-adhesion [41].

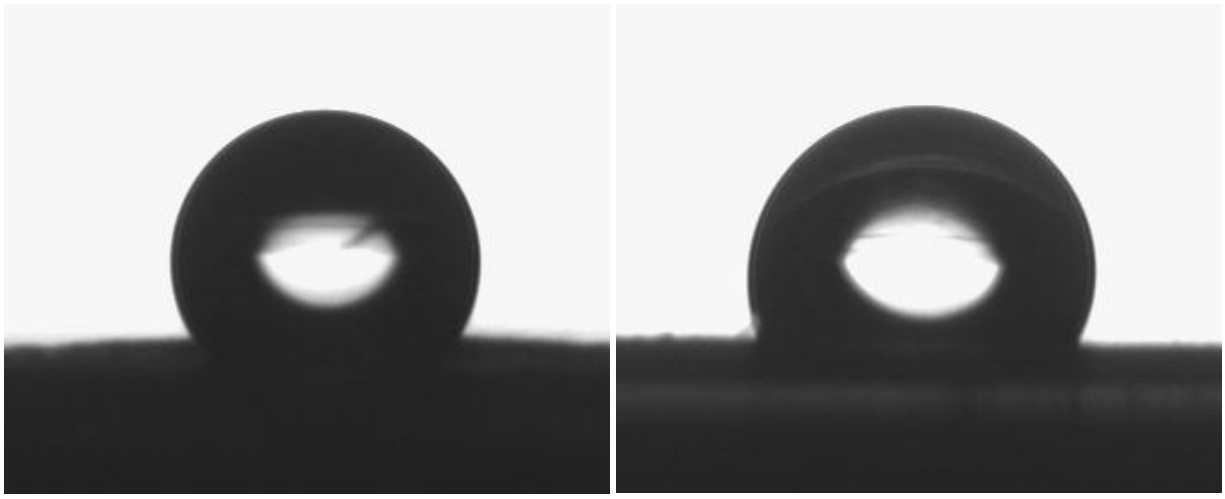

Fig 2. Two different droplets of deionized water deposited on the PLA scaffold.

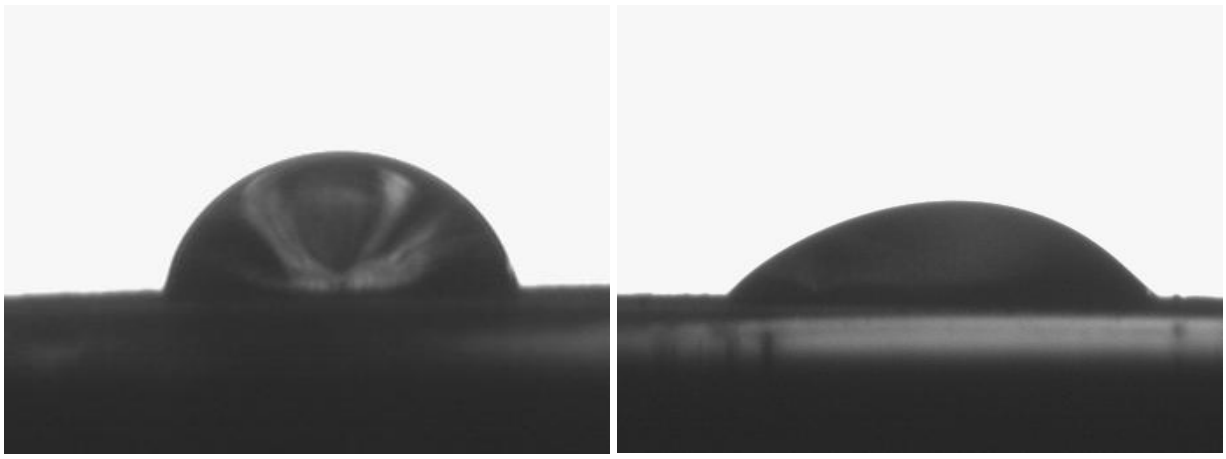

Fig. 3. Droplets of deionized water deposited on the SS:PEO side of the bilayer scaffolds with the 2:4 ratio SS:PEO (left) and the 1.2:4 ratio SS:PEO (right).

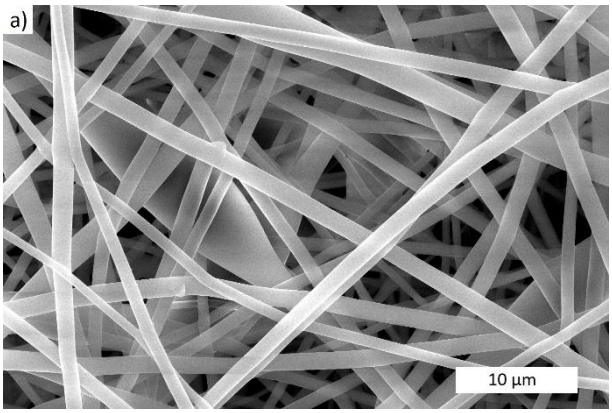
a)
10 µm

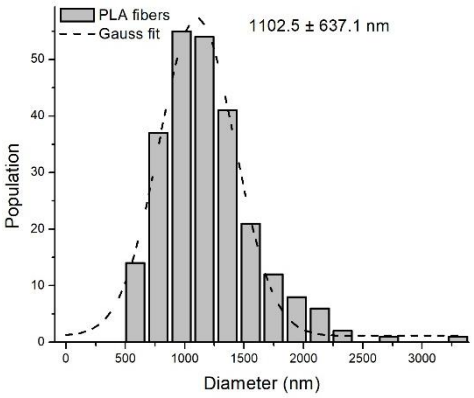
PLA fibers
Gauss fit
1102.5 ± 637.1 nm
Population
Diameter (nm)

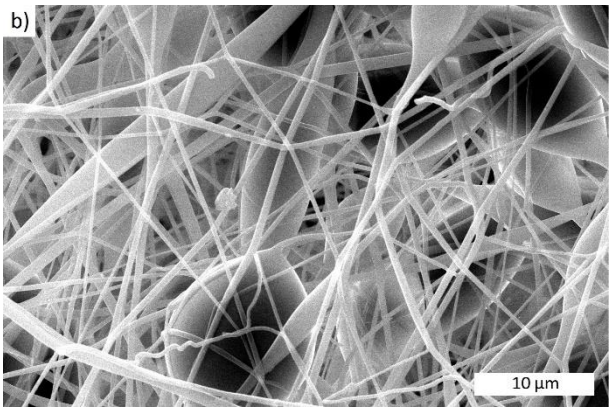
b)
10 µm

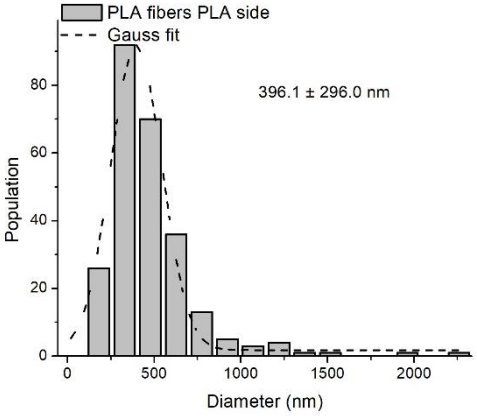
PLA fibers PLA side
Gauss fit
396.1 ± 296.0 nm
Population
Diameter (nm)

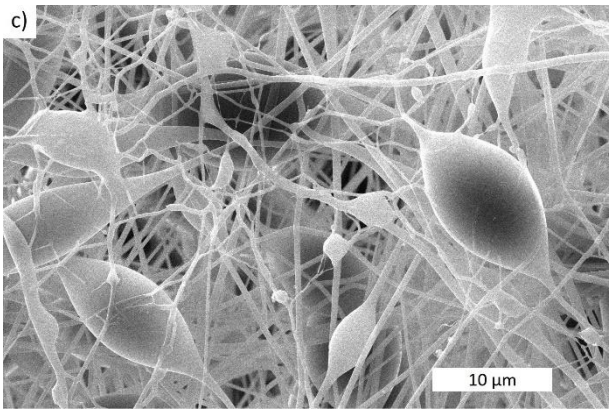
c)
10 µm

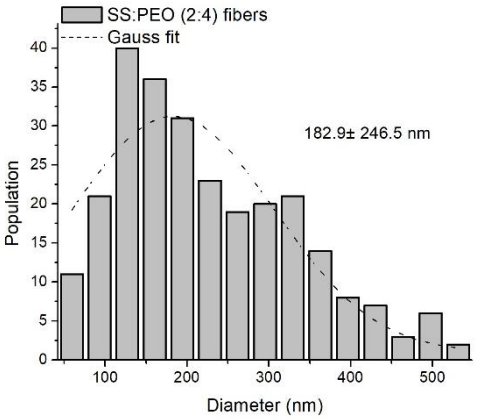
SS:PEO (2:4) fibers
Gauss fit
182.9± 246.5 nm
Population
Diameter (nm)

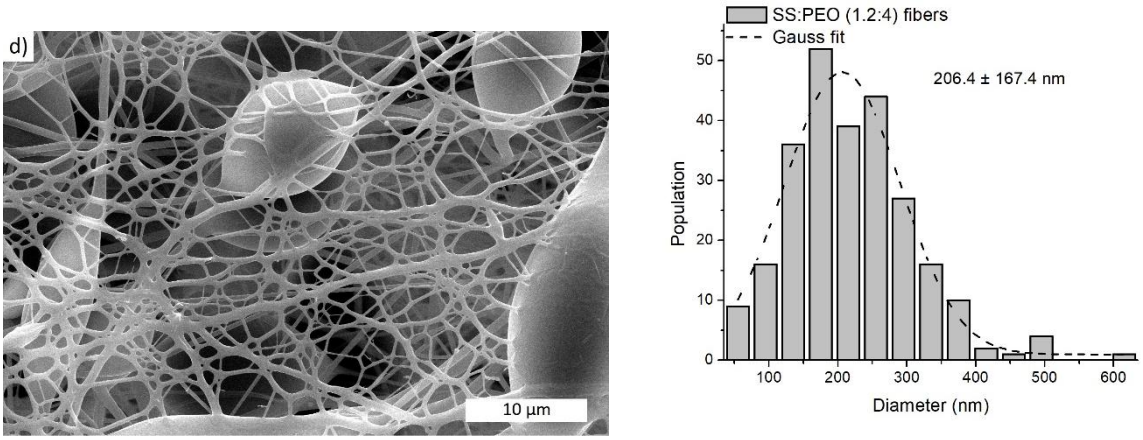

Fig. 4. SEM Micrographs and the according size distribution of a) PLA fibers b) PLA fibers in the bilayer scaffolds, c) SS:PEO (1:2) fibers in the bilayer scaffold and d) the SS:PEO (1.2:4) fibers in the bilayer scaffold.

XRD and FTIR analysis of the scaffolds have been studied for each part of the bilayer scaffolds when it was possible (**Fig. 5** and **Fig. 6**). XRD of the PLA show broad hallows, confirming the amorphous phase of the electrospun fibers. Contrary to the PLA, the XRD analysis of the PEO before and after electrospinning shows the characteristic peaks of the crystalline (electrospun or not) PEO (**Fig. 5.b** and **Fig. SI. 2**). Difference of the peaks ratios at 19 ° and 23 ° can be attributed to a crystalline structure because of the elongation of the PEO into fibers [42]. Finally, XRD analysis of the bilayer witth the SS:PEO side on top displayed an amourphous broad hallow of the PLA (**Fig. 5.a** and **Fig. 5.c**) with two characteristic peaks of the electrospinned PEO scaffold at 19 ° and 23 °. This observation is evidence of the presence of crystalline peaks in both bilayer scaffolds, which consists of the second proof of the successfully electrospun bilayer (**Fig. 5.d**). Then, the intensity of the PEO peaks of the bilayer scaffolds can be representative of the quantity of SS:PEO fibers that have been successfully deposited on the sturdy PLA scaffold. Weak intensity for the 1:2 SS:PEO fibers compared to the very intense 1.2:4 SS:PEO fibers is correlated with the SEM observations in **Fig. 4.** Microstructure of the bilayer containing 1.2:4 SS:PEO fiber displays a much better repartition and coverage of fibers compared to the bilayer containing 1.2: SS:PEO fiber.

a)

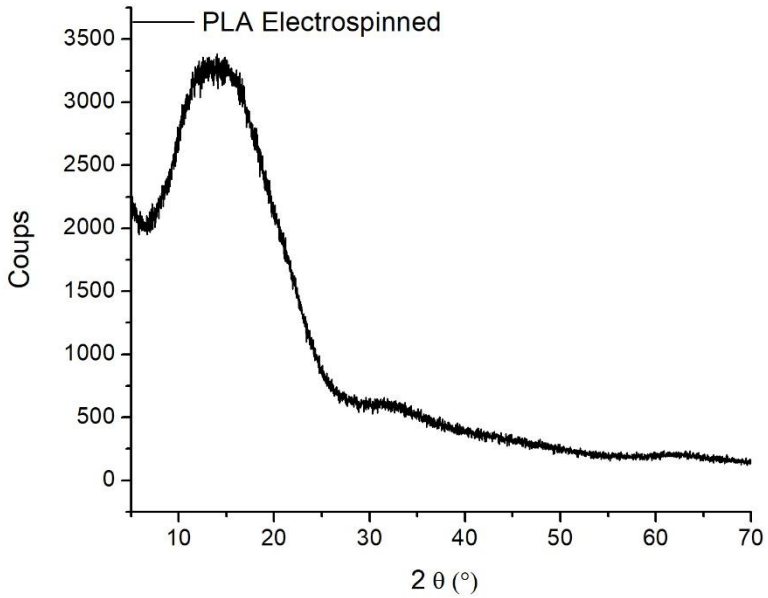
PLA Electrospinned
Coups
3500
3000
2500
2000
1500
1000
500
0
10
20
30
40
50
60
70
2 θ (°)

b)

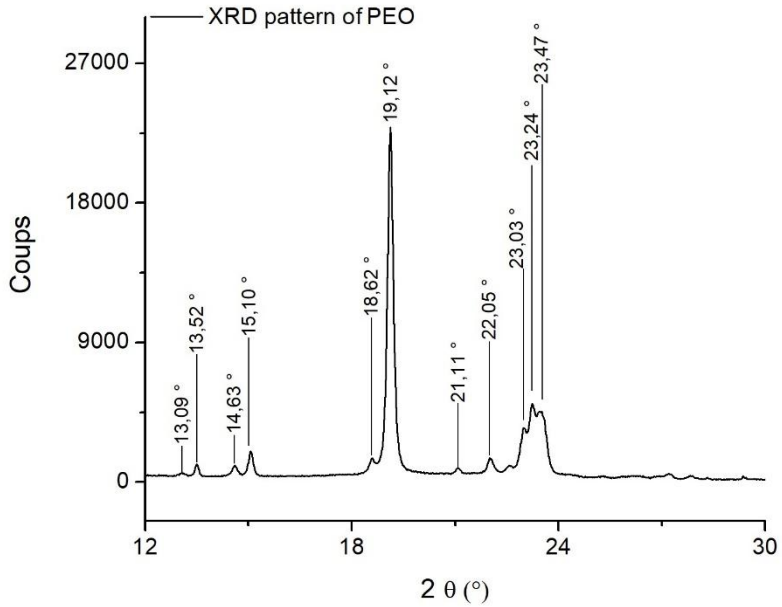
XRD pattern of PEO
Coups
27000
18000
9000
0
12
18
24
30
2 θ (°)
13,09 °
13,52 °
14,63 °
15,10 °
18,62 °
19,12 °
21,11 °
22,05 °
23,03 °
23,24 °
23,47 °

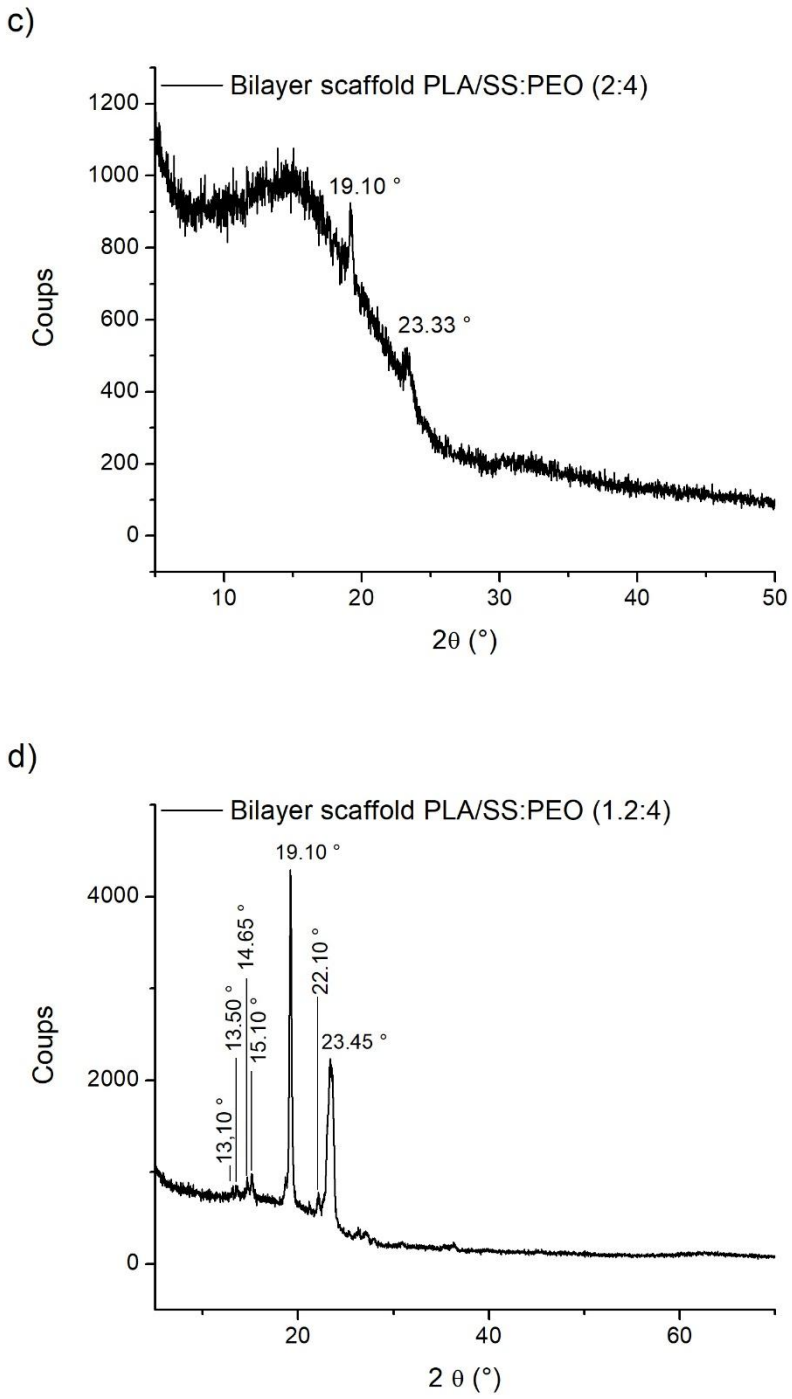

Fig. 5. XRD patterns of a) electrospinned PLA (25% w/v), b) electrospinned PEO (5% w/v), c) electrospun bilayer scaffolds with PLA/SS:PEO (2:4) fibers and d) bilayer scaffolds with PLA/SS:PEO (1.2:4) fibers .

FTIR analysis of the electrospun PLA fibers displays the characteristic vibration band of the esters at 1750 cm^{-1}. Moreover, the absence of the vibration band of the O-H bonds between 3000 cm^{-1} and 3500 cm^{-1} in the FTIR spectra (**Fig. 6.b**) confirms the absence of TFE in the fibers. The FTIR spectra

of the SS:PEO fibers show the presence of PEO with a broad vibration band centered at 2882 cm^{-1} as well as the SS characteristic vibration bands at 1522 cm^{-1} and 1644 cm^{-1} (amides)(**Fig. 6.a**). FTIR analysis of the PLA/SS:PEO bilayer scaffolds have then been undertaken side and one spectra on the PLA side. The FTIR analysis of the SS:PEO side show the characteristic vibration bands of SS and PEO while the FTIR spectra of the PLA side shows the vibration bands of only the PLA with the C=O of the esters at 1750 cm^{-1} (**Fig. 6.b**). These results confirms the bilayer structure of the scaffolds with the absence of the SS:PEO signals on the PLA side of the scaffolds, and the presence of the typical XRD peaks and FTIR vibration bands of the PEO when the scaffold is analyzed on the SS side.

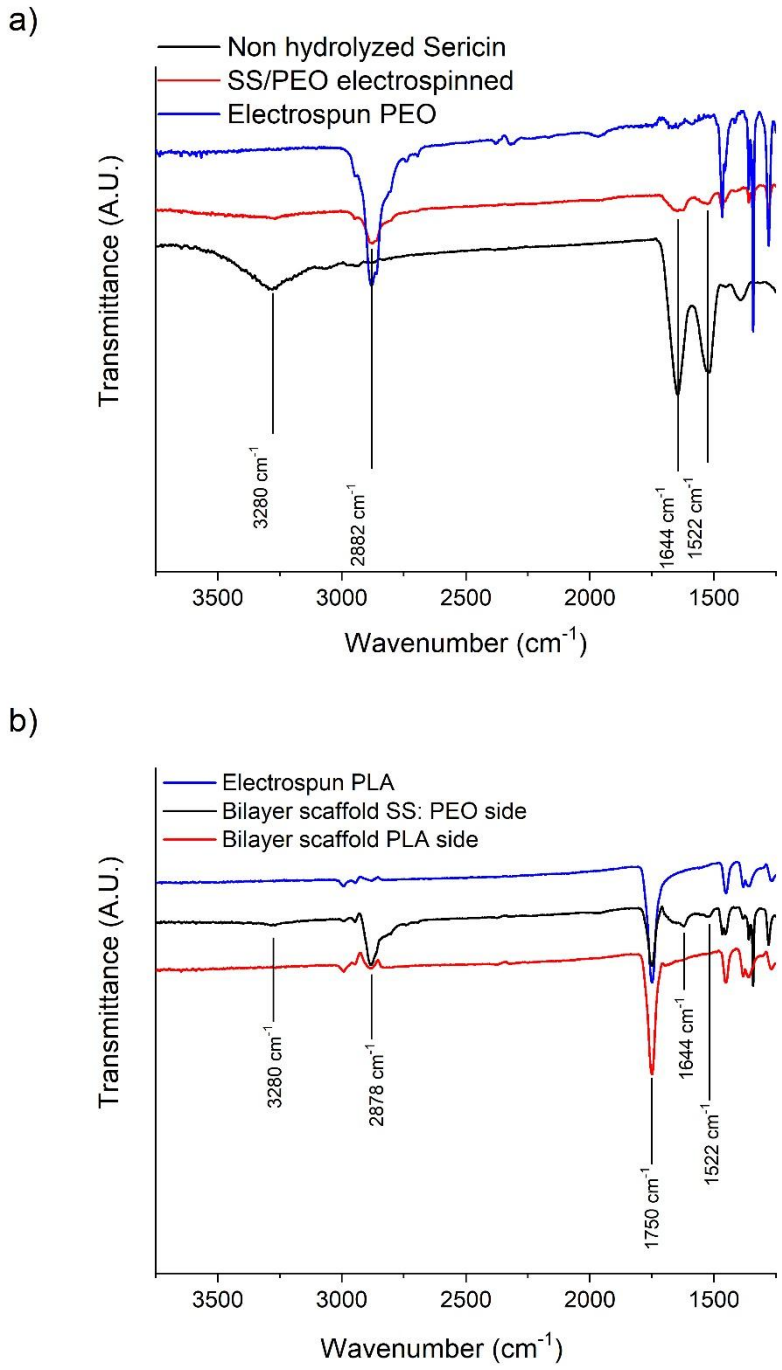

Fig. 6. ATR-IR spectra of a) non-hydrolyzed SS with SS:PEO (ratio 1.2:4) fibers, b) bilayer scaffolds compared to pure electrospun PLA.

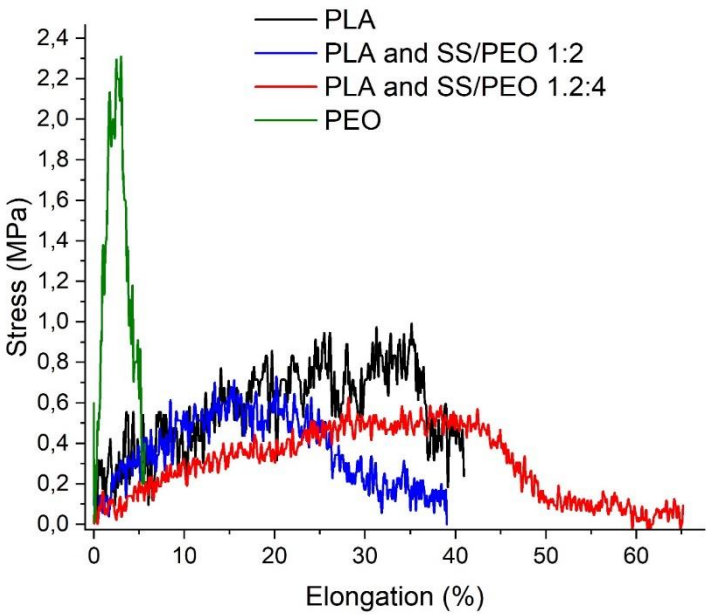

Fig. 7. Mechanical tests of PEO, PLA, PLA with SS:PEO 1.2:4 and PLA with SS:PEO 1:2.

Table 2. Young's Modulus, maximum stress and elongation at break of the different scaffolds.

Scaffold	*Young's modulus*	*Maximum stress*	*Elongation at break*
PEO	*0.97 ± 0.10 MPa*	*2.3 MPa*	*5 %*
PLA	*0.025 ± 1.5 10^{-3} MPa*	*0.95 MPa*	*37 %*
PLA and SS:PEO (1.2:4)	*0.024 ± 1.1 10^{-3} MPa*	*0.68 MPa*	*45 %*
PLA and SS:PEO (1:2)	*0.016 ± 5.6 10^{-4} MPa*	*0.56 MPa*	*25 %*

Mechanical resistance to stress has been assessed to study the differences between the different electrospinned scaffolds, mono- or bi-layers. Mechanical tests were run on a tensile micromachine (DEBEN microtest system) using stripes of each scaffold. The results are presented in **Fig. 7** and **Table 2**. As we are using porous scaffolds, our test are not meant to deliver quantitative mechanical parameters, but they are used for a qualitative comparison. We observe that the pure PEO scaffolds are rigid and break easily after a 5% strain. The rigidity of the PEO scaffold is the result of its high crystallinity obsverved in XRD (**Fig. 5.b**). Pure PLA scaffolds are more elastic and the deformation at

break increased compared to pure PEO (up to 37 % of elongation). For the bilayer scaffolds, SS:PEO (1:2) fibers on the PLA scaffolds decreased the mechanical strength of the scaffold, reducing its elongation at break from 37 % to 25 %, without interferring with the flexibility of the PLA. However this can be explained by the low SS:PEO fibers quantity observed in the SEM images (**Fig. 4.c**) as well as the weak peaks in XRD analysis (**Fig. 5.c**). ES of SS:PEO 1.2:4 fibers on the PLA scaffolds decreased the mechanical strength of the scaffold with an increase of the flexibility. The miscrostructure observed in SEM micrograhs, and the more intense peaks in XRD analysis suggests a higher content of SS:PEO (1.2:4) fibers than the SS:PEO (1:2) fibers in the bilayer scaffold. These results are comparable with the observations made by Bakhsheshi *et al.* [25] on PVA/CS/Sericin fibers. Increasing the content of sericin weakens the strength and increases the flexibility of the scaffolds.

4. Conclusions

Non-hydrolyzed SS was successfully electrospinned in the presence of PEO with ratios from 1.2:4 to 1:2 (SS:PEO) in water, yielding nanometric fibers with a size diameter ranging from 100 nm and 150 nm. Those fragile and sticky fibers, once electrospinned directly on PLA films constituted of 300 nm to 400 nm fibers lead to the fabrication of bilayer scaffolds, allowing the manipulation of very fine SS constituted fibers. Analysis by XRD, IR, SEM and mechanical properties shown that electrospinning of SS:PEO fibers on the PLA was successful, and yielded to the obtention of bilayered scaffolds. Those scaffolds display a hydrophobic side due to the presence of PLA and a hydrophilic side due to the presence of SS:PEO fibers on the other side. Adjustable wettability of one side of the scaffold can be used for various applications such as the biomedical field and bio-adhesion. Although PLA fibers shows defects and SS:PEO fibers coverage in not optimal an optimization of the electrospinning process as well as an improvement of the production speed is currently studied and could lead to larger scale fabrication. Tests of the cytotoxicity of the fibers will be undertaken as well as their performance for different applications such as tissue engineering, cell culture and anti-microbial activity.

Acknowledgement

The authors highly acknowledge the financial support from the Initiative MSTD and the Alliance Sorbonne Université. The authors highly acknowledge the Service d'Analyses Physico-Chimiques of the UTC (SAPC) for the help provided and the analysis they performed for this research paper (especially Caroline Lefèbvre, François Oudet, and Frédéric Nadaud).

References

1. Reneker, D.H.; Chun, I. Nanometre Diameter Fibres of Polymer, Produced by Electrospinning, *Nanotechnology*, **1996**, *7*, 216–223, doi:10.1088/0957-4484/7/3/009.
2. Rho, K.S.; Jeong, L.; Lee, G.; Seo, B.-M.; Park, Y.J.; Hong, S.-D.; Roh, S.; Cho, J.J.; Park, W.H.; Min, B.-M. Electrospinning of Collagen Nanofibers: Effects on the Behavior of Normal Human Keratinocytes and Early-Stage Wound Healing, *Biomaterials*, **2006**, *27*, 1452–1461, doi:10.1016/j.biomaterials.2005.08.004.
3. Saraiva, S.; Pereira, P.; Paula, C.T.; Rebelo, R.C.; Coelho, J.F.J.; Serra, A.C.; Fonseca, A.C. Development of Electrospun Mats Based on Hydrophobic Hydroxypropyl Cellulose Derivatives, *Materials Science and Engineering: C*, **2021**, *131*, 112498, doi:10.1016/j.msec.2021.112498.
4. Lin, W.; Chen, M.; Qu, T.; Li, J.; Man, Y. Three-dimensional Electrospun Nanofibrous Scaffolds for Bone Tissue Engineering, *J Biomed Mater Res*, **2020**, *108*, 1311–1321, doi:10.1002/jbm.b.34479.
5. Zhang, C.; Zhang, D.; Chen, D.; Li, M. A Bilayered Scaffold Based on RGD Recombinant Spider Silk Proteins for Small Diameter Tissue Engineering. *Polym. Compos.,* **2016**, *37*, 523–531, doi:10.1002/pc.23208.
6. Shi, X.; Zhou, W.; Ma, D.; Ma, Q.; Bridges, D.; Ma, Y.; Hu, A. Electrospinning of Nanofibers and Their Applications for Energy Devices, *Journal of Nanomaterials,* **2015**, *2015*, 1–20, doi:10.1155/2015/140716.
7. Parsaei, S.; Zebarjad, S.M.; Moghim, M.H. Fabrication and Post-processing of PI / PVDF-HFP / PI Electrospun Sandwich Separators for Lithium-ion Batteries, *Polymer Engineering & Sci,* **2022**, *62*, 3641–3651, doi:10.1002/pen.26133.
8. Seeram Ramakrishna; Zamani, M.; Molamma P Prabhakaran Advances in Drug Delivery via Electrospun and Electrosprayed Nanomaterials, *IJN,* **2013**, 2997, doi :10.2147/IJN.S43575.
9. Ghafouri, S.E. ; Mousavi, S.R. ; Khakestani, M. ; Mozaffari, S. ; Ajami, N. ; Khonakdar, H.A. Electrospun Nanofibers of Poly (Lactic Acid)/Poly (ε -caprolactone) Blend for the Controlled Release of Levetiracetam, *Polymer Engineering & Sci,* **2022**, pen.26167, doi:10.1002/pen.26167.
10. Zhang, Z.; Ji, D.; He, H.; Ramakrishna, S. Electrospun Ultrafine Fibers for Advanced Face Masks, *Materials Science and Engineering: R: Reports* **2021**, *143*, 100594, doi:10.1016/j.mser.2020.100594.
11. Oğlakcıoğlu, N.; Akduman, C.; Sarı, B. Investigation of Thermal Comfort Properties of Electrospun Thermoplastic Polyurethane Fiber Coated Knitted Fabrics for Wind-resistant Clothing, *Polym Eng Sci,* **2021**, *61*, 669–679, doi:10.1002/pen.25607.
12. Li, Y.; Yin, X.; Yu, J.; Ding, B. Electrospun Nanofibers for High-Performance Air Filtration, *Composites Communications,* **2019**, *15*, 6–19, doi:10.1016/j.coco.2019.06.003.
13. Bhardwaj, N.; Kundu, S.C. Electrospinning: A Fascinating Fiber Fabrication Technique, *Biotechnology Advances,* **2010**, *28*, 325–347, doi:10.1016/j.biotechadv.2010.01.004.
14. Khajavi, R.; Abbasipour, M. Electrospinning as a Versatile Method for Fabricating Coreshell, Hollow and Porous Nanofibers, *Scientia Iranica,* **2012**, *19*, 2029–2034, doi:10.1016/j.scient.2012.10.037.
15. Leon-Valdivieso, C.Y.; Garcia-Garcia, A.; Legallais, C.; Bedoui, F. Electrospinning of Biomedically Relevant Multi-Region Scaffolds: From Honeycomb to Randomly-Oriented Microstructure, *Polymer,* **2020**, *202*, 122606, doi:10.1016/j.polymer.2020.122606.
16. Mehta, P.P.; Pawar, V.S. Electrospun Nanofiber Scaffolds, In *Applications of Nanocomposite Materials in Drug Delivery*, Elsevier, 2018; pp. 509–573 ISBN 978-0-12-813741-3.
17. Arango, M.C.; Montoya, Y.; Peresin, M.S.; Bustamante, J.; Álvarez-López, C. Silk Sericin as a Biomaterial for Tissue Engineering: A Review, *International Journal of Polymeric Materials and Polymeric Biomaterials,* **2021**, *70*, 1115–1129, doi:10.1080/00914037.2020.1785454.
18. Belbéoch, C.; Lejeune, J.; Vroman, P.; Salaün, F. Silkworm and Spider Silk Electrospinning: A Review, *Environ Chem Lett,* **2021**, *19*, 1737–1763, doi:10.1007/s10311-020-01147-x.
19. Sarovart, S.; Sudatis, B.; Meesilpa, P.; Grady, B.P.; Magaraphan, R. The Use of Sericin as an Antioxidant and Antimicrobial for Polluted Air Treatment, *Reviews on Advanced Materials Science*, **2003**, *5*, 193–198.

20. Purwar, R.; Sai Goutham, K.; Srivastava, C.M. Electrospun Sericin/PVA/Clay Nanofibrous Mats for Antimicrobial Air Filtration Mask, *Fibers Polym*, **2016**, *17*, 1206–1216, doi:10.1007/s12221-016-6345-7.
21. Purwar, R.; Verma, A.; Batra, R. Antimicrobial Gelatin/Sericin/Clay Films for Packaging of Hygiene Products, *Journal of Polymer Engineering*, **2019**, *39*, 744–751, doi:10.1515/polyeng-2018-0406.
22. Zhang, Y.-Q.; Ma, Y.; Xia, Y.-Y.; Shen, W.-D.; Mao, J.-P.; Xue, R.-Y. Silk Sericin–Insulin Bioconjugates: Synthesis, Characterization and Biological Activity, *Journal of Controlled Release*, **2006**, *115*, 307–315, doi:10.1016/j.jconrel.2006.08.019.
23. Zhaorigetu, S.; Sasaki, M.; Watanabe, H.; Kato, N. Supplemental Silk Protein, Sericin, Suppresses Colon Tumorigenesis in 1,2-Dimethylhydrazine-Treated Mice by Reducing Oxidative Stress and Cell Proliferation, *Bioscience, Biotechnology, and Biochemistry*, **2001**, *65*, 2181–2186, doi:10.1271/bbb.65.2181.
24. Sapru, S.; Das, S.; Mandal, M.; Ghosh, A.K.; Kundu, S.C. Prospects of Nonmulberry Silk Protein Sericin-Based Nanofibrous Matrices for Wound Healing – In Vitro and in Vivo Investigations, *Acta Biomaterialia*, **2018**, *78*, 137–150, doi:10.1016/j.actbio.2018.07.047.
25. Bakhsheshi-Rad, H.R.; Ismail, A.F.; Aziz, M.; Akbari, M.; Hadisi, Z.; Omidi, M.; Chen, X. Development of the PVA/CS Nanofibers Containing Silk Protein Sericin as a Wound Dressing: In Vitro and in Vivo Assessment, *International Journal of Biological Macromolecules*, **2020**, *149*, 513–521, doi:10.1016/j.ijbiomac.2020.01.139.
26. Zhang, X.H.; Tsukada, M.; Satoh, Y.; Morikawa, H. Production of Silk Sericin Nanofibers, *AMR*, **2011**, *175–176*, 348–352, doi:10.4028/www.scientific.net/AMR.175-176.348.
27. Belda Martin, C. Silk Bionanocomposites :Design, Characterization and Potential Applications, Université de Technologie de Compiègne: Compiègne, **2020**.
28. Eslah, S.; Tavanai, H.; Morshed, M. Electrospinning and Characterization of Poly (Vinyl Alcohol)–Sericin Nanofibers as a Potential for Tissue Engineering Applications, *The Journal of The Textile Institute*, **2015**, 1–9, doi:10.1080/00405000.2015.1072328.
29. Zhou, C.-J.; Li, Y.; Yao, S.-W.; He, J.-H. Silkworm-Based Silk Fibers by Electrospinning, *Results in Physics*, **2019**, *15*, 102646, doi:10.1016/j.rinp.2019.102646.
30. He, H.; Cai, R.; Wang, Y.; Tao, G.; Guo, P.; Zuo, H.; Chen, L.; Liu, X.; Zhao, P.; Xia, Q. Preparation and Characterization of Silk Sericin/PVA Blend Film with Silver Nanoparticles for Potential Antimicrobial Application, *International Journal of Biological Macromolecules*, **2017**, *104*, 457–464, doi:10.1016/j.ijbiomac.2017.06.009.
31. Zhang, Y.-Q. Applications of Natural Silk Protein Sericin in Biomaterials, *Biotechnology Advances*, **2002**, *20*, 91–100, doi:10.1016/S0734-9750(02)00003-4.
32. Gupta, D.; Agrawal, A.; Rangi, A. Extraction and Characterization of Silk Sericin, *Indian J. Fibre Text. Res.*, **2014**, 10.
33. Gulrajani, M.L.; Purwar, R.; Prasad, R.K.; Joshi, M. Studies on Structural and Functional Properties of Sericin Recovered from Silk Degumming Liquor by Membrane Technology, *J. Appl. Polym. Sci.* , **2009**, *113*, 2796–2804, doi:10.1002/app.29925.
34. Bascou, R.; Hardouin, J.; Ben Mlouka, M.A.; Guénin, E.; Nesterenko, A. Detailed Investigation on New Chemical-Free Methods for Silk Sericin Extraction, *Materials Today Communications*, **2022**, *33*, 104491, doi:10.1016/j.mtcomm.2022.104491.
35. Jacobs, V.; Anandjiwala, R.D.; Maaza, M. The Influence of Electrospinning Parameters on the Structural Morphology and Diameter of Electrospun Nanofibers, *J. Appl. Polym. Sci*, **2010**, *115*, 3130–3136, doi:10.1002/app.31396.
36. Bernardo, M.P.; da Silva, B.C.R.; Hamouda, A.E.I.; de Toledo, M.A.S.; Schalla, C.; Rütten, S.; Goetzke, R.; Mattoso, L.H.C.; Zenke, M.; Sechi, A. PLA/Hydroxyapatite Scaffolds Exhibit in Vitro Immunological Inertness and Promote Robust Osteogenic Differentiation of Human Mesenchymal Stem Cells without Osteogenic Stimuli, *Sci Rep*, **2022**, *12*, 2333, doi:10.1038/s41598-022-05207-w.
37. Areias, A.C.; Ribeiro, C.; Sencadas, V.; Garcia-Giralt, N.; Diez-Perez, A.; Gómez Ribelles, J.L.; Lanceros-Méndez, S. Influence of Crystallinity and Fiber Orientation on Hydrophobicity and Biological Response of Poly(l-Lactide) Electrospun Mats, *Soft Matter*, **2012**, *8*, 5818, doi:10.1039/c2sm25557j.

38. Casasola, R.; Thomas, N.L.; Trybala, A.; Georgiadou, S. Electrospun Poly Lactic Acid (PLA) Fibres: Effect of Different Solvent Systems on Fibre Morphology and Diameter, *Polymer*, **2014**, *55*, 4728–4737, doi:10.1016/j.polymer.2014.06.032.
39. Gómez-Pachón, E.Y.; Vera-Graziano, R.; Campos, R.M. Structure of Poly(Lactic-Acid) PLA Nanofibers Scaffolds Prepared by Electrospinning, *IOP Conf. Ser.: Mater. Sci. Eng.* , **2014**, *59*, 012003, doi:10.1088/1757-899X/59/1/012003.
40. Zhao, R.; Li, X.; Sun, B.; Tong, Y.; Jiang, Z.; Wang, C. Nitrofurazone-Loaded Electrospun PLLA/Sericin-Based Dual-Layer Fiber Mats for Wound Dressing Applications, *RSC Adv.* , **2015**, *5*, 16940–16949, doi:10.1039/C4RA16208K.
41. Dou, X.-Q.; Zhang, D.; Feng, C.; Jiang, L. Bioinspired Hierarchical Surface Structures with Tunable Wettability for Regulating Bacteria Adhesion, *ACS Nano*, **2015**, *9*, 10664–10672, doi:10.1021/acsnano.5b04231.
42. Mishra, S.R.; Ranjith, K.; Swathi, S.K.; Ramamurthy, P.C. Nanostructured Barbed Wire Architecturing of Organic Conducting Material Blends by Electrospinning, *Appl. Phys. Lett.*, **2012**, *100*, 013302, doi:10.1063/1.3673620.